Variability of primary production and air-sea CO_2 flux in the Southern Ocean

Shanlin Wang[1] and J. Keith Moore[1]

Received 29 October 2010; revised 18 May 2011; accepted 5 November 2011; published 24 January 2012.

[1] Biogeochemical cycling in the Southern Ocean (SO) plays a key role in the global sea-air CO_2 balance and in the ocean anthropogenic carbon inventory (Ito et al., 2010; Khatiwala et al., 2009; Sarmiento et al., 2004). Some previous studies suggest a decreasing trend in the Southern Ocean carbon sink (Le Quéré et al., 2007; Lovenduski et al., 2007; Wetzel et al., 2005). We investigate the interannual and decadal variations in sea-air CO_2 flux and phytoplankton production in the SO with hindcast simulations by an ocean biogeochemical model. Decreasing trends in sinking POC and primary production are found from 1979 to 2003, concurrent with a decreasing trend in carbon uptake from the atmosphere. Simulations show substantial interannual and decadal variability in productivity. The sea-air CO_2 flux is significantly correlated with sinking POC, especially in high productivity regions of the Southern Ocean. Both mixed layer depths and iron concentrations are important to the long-term trends in production and phytoplankton community structure. Sea ice cover also plays an important role at high latitudes. Variability in dust deposition in recent decades has little influence on total SO productivity and carbon uptake, however, there are regional impacts near dust source regions. Accurately representing mixed layer depths and their impacts on phytoplankton light stress are critical for understanding how climate change impacts SO ecosystems and biogeochemistry.

Citation: Wang, S., and J. K. Moore (2012), Variability of primary production and air-sea CO_2 flux in the Southern Ocean, *Global Biogeochem. Cycles*, *26*, GB1008, doi:10.1029/2010GB003981.

1. Introduction

[2] The Southern Ocean (SO) has been recognized as a key region for the global carbon cycle, accounting for ~40% of the anthropogenic CO_2 sink [*Gruber et al.*, 2009; *Khatiwala et al.*, 2009; *Sabine et al.*, 2004]. A comprehensive understanding of the SO carbon sink and controlling mechanisms is crucial for better prediction of changes in global carbon inventories and climate. Previous studies suggested that SO climate dynamics have been changing in recent decades. A positive trend in the index of the Southern Annular Mode (SAM), associated with a strengthening of westerly winds, was observed [*Archer and Caldeira*, 2008; *Cai*, 2006; *Thompson et al.*, 2000]. Observations also show a major warming over the Antarctic Peninsula and Patagonia, and a cooling over eastern Antarctica and the Antarctic plateau [*Comiso*, 2000; *Thompson and Solomon*, 2002; *Turner et al.*, 2005]. Warming has spread over the upper SO, especially within the Antarctic Circumpolar Current (ACC), consistent with a poleward migration of the ACC [*Gille*, 2008]. *Comiso and Nishio* [2008] estimated an overall weak positive trend in Southern Hemisphere sea ice extent, with decreasing ice in the Bellingshausen/Amundsen Sea. It is likely that these changes in heat and freshwater flux, and in atmospheric circulation have led to changes in ocean mixing and circulation, such as the observed variations in ocean transport through Drake Passage [*Meredith et al.*, 2004] and a simulated increase in Agulhas leakage in response to changes in the SAM [*Biastoch et al.*, 2009]. Quantification of the SO carbon sink, including its spatial patterns and trends, have been the focus of several recent studies. Much of the SO anthropogenic carbon storage was related to intermediate water formation, leading to high, vertically integrated CO_2 concentrations between 14°S–50°S [*Ito et al.*, 2010; *Khatiwala et al.*, 2009; *Sabine et al.*, 2004]. Ocean in situ carbon dioxide observations showed a reduction in the carbon sink in the Indian sector of the SO over the past two decades [*Metzl*, 2009]. A number of model studies also suggested that the SO carbon sink had showed a weakening trend over the past few decades [*Le Quéré et al.*, 2007; *Lovenduski et al.*, 2007, 2008; *Wetzel et al.*, 2005]. Model simulations and observations showed a positive correlation between the CO_2 flux trend and the increasing westerly winds, which suggested that the weakening of the carbon sink was associated with changes in physical mixing and upwelling [*Le Quéré et al.*, 2007; *Lovenduski et al.*, 2007, 2008; *Metzl*, 2009]. Other studies suggested that the effects of heat and freshwater flux changes on CO_2 flux were compensated by the effects of increasing wind speed and

[1]Earth System Science, University of California, Irvine, Irvine, California, USA.

0886-6236/12/2010GB003981

resulted in no robust trends [*Law et al.*, 2008; *Matear and Lenton*, 2008].

[3] Over long time scales, export production is important for the SO carbon inventory. Surface nutrient consumption in the SO also likely influences nutrient concentrations and phytoplankton productivity at low latitudes, through lateral transport [*Marinov et al.*, 2006; *Sarmiento et al.*, 2004; *Toggweiler et al.*, 1991]. Oceanic primary productivity is sensitive to the variability in physical forcing and nutrient supply associated with climate change. Many observations have shown interannual, and regional variability in phytoplankton community composition, biomass and productivity [*Arrigo et al.*, 2008; *Prézelin et al.*, 2004; *Smith and Comiso*, 2008]. Some of this variability was related to physical forcing, such as changes in the SAM and sea ice dynamics [*Arrigo et al.*, 2008; *Smith and Comiso*, 2008; *Vernet et al.*, 2008]. Nutrient supply, especially iron, also plays a key role in modulation of SO production [i.e., *Moore and Abbott*, 2000]. Changes in physical fields, such as wind speed, sea surface temperature and freshwater flux, can alter ocean stratification, mixed layer depths, mixing and upwelling, which impacts nutrient distributions. Dust deposition, an important source of iron, has increased over the 20th century [*Mahowald et al.*, 2010]. It was suggested that dust storms in the Australian sector of the SO had resulted in significant elevations of phytoplankton abundance and a strong CO_2 drawdown was associated with the dust events [*Gabric et al.*, 2010]. Other studies also highlighted the importance of dust deposition in phytoplankton carbon fixation and interannual variations in air-sea CO_2 fluxes in the SO [*Cassar et al.*, 2007; *Patra et al.*, 2007]. Recent modeling results suggested that Southern Ocean biogeochemistry was more heavily influenced by sedimentary iron sources than dust deposition [*Moore and Braucher*, 2008; *Tagliabue et al.*, 2010].

[4] Though satellite data in the past decade showed no overall trend of annual primary production in the Southern Ocean [*Arrigo et al.*, 2008; *Behrenfeld et al.*, 2006], there were some regional productivity changes [*Behrenfeld et al.*, 2006]. A number of studies have shown substantial changes in ecosystem composition [e.g., *Brierley and Kingsford*, 2009; *Montes-Hugo et al.*, 2009; *Ross et al.*, 2008]. *Montes-Hugo et al.* [2009] found the summertime surface chlorophyll declined by 12% along the western Antarctic Peninsula over the past three decades, but there was no simple relationship between variations in community structure, productivity and physical forcing. It is necessary to investigate variability of phytoplankton community and productivity, and related impacts on the carbon cycle over longer time scales. Model simulations are a useful complementary method to study those variations in production, to understand the driving mechanisms, and to assess the consequences for biogeochemical cycles.

[5] This work involves examining the relative impacts of variations in wind speed, sea surface temperature, photosynthetically available radiation (PAR), mixed layer depth, and sea ice cover on phytoplankton community composition, primary and export production, and impacts of biological production on air-sea CO_2 exchange in the SO with hindcast simulations. The Biogeochemical Elemental Cycling (BEC) model [*Moore et al.*, 2004] was also used by *Lovenduski et al.* [2007, 2008] to study SO biogeochemistry. Here the BEC model has been modified to better study the SO. The current model has incorporated *Phaeocystis* as an additional phytoplankton functional group, and employed a more realistic sedimentary iron field [*Moore and Braucher*, 2008; *Wang and Moore*, 2011]. Reconstructed dust deposition in the second half of the 20th century [*Mahowald et al.*, 2010] is used to investigate dust impacts on the SO.

2. Methods

[6] We used a state-of-the-art ocean biogeochemical/ecosystem model, the BEC model, [*Moore et al.*, 2002, 2004] to study the SO. The BEC model runs within the coarse resolution, ocean circulation component of the National Center for Atmospheric Research (NCAR) Community Climate System Model 3.1 (CCSM3) [*Collins et al.*, 2006; *Yeager et al.*, 2006]. The model includes 25 vertical levels. There are 100 × 116 horizontal grid points, with a longitudinal resolution of 3.6° and varying latitudinal resolutions of 0.9°–2.0°. Our focus in this work is the Southern Ocean (>35°S). The wind speed-mixing relation in the model was adjusted to better match the observed mixed layer depths in the Southern Ocean [*de Boyer Montégut et al.*, 2004]. The mixed layer depths tend to be much too shallow in CCSM3.1 [*Doney et al.*, 2009b], however the bias of mixed layer depth has been significantly reduced in our simulations, and mean mixed layer depths for the current SO are in good agreement with the observations [*Wang and Moore*, 2011]. The bias in monthly mean mixed layer depth was reduced from 18 m too shallow in the standard CCSM 3.1 model to a bias of +2 m [*Wang and Moore*, 2011].

[7] The BEC model used here includes five phytoplankton functional groups, one zooplankton group and biogeochemical cycling of multiple growth limiting nutrients (nitrate, ammonium, phosphate, iron and silicate) [*Moore et al.*, 2004; *Wang and Moore*, 2011]. The five phytoplankton groups were diatoms, diazotrophs, small phytoplankton, coccolithophores and *Phaeocystis*. *Phaeocystis* was recently added to the BEC model, based on observed features of *Phaeocystis antarctica* colonies [*Wang and Moore*, 2011]. It has been reported that both *Phaeocystis* and diatoms are major blooming species in the SO [i.e., *DiTullio et al.*, 2000; *Feng et al.*, 2010; *Poulton et al.*, 2007; *Smith and Asper*, 2001]. *Phaeocystis* generally account for less production than diatoms; however, they can compete with diatoms and sometimes become the dominant phytoplankton group [i.e., *Peloquin and Smith*, 2007; *Poulton et al.*, 2007; *Smith et al.*, 1999; *Tang et al.*, 2009]. In the BEC model, both diatoms and *Phaeocystis* represent larger phytoplankton, which often dominate in more nutrient-rich waters and export carbon more efficiently. Compared to the diatom group, the *Phaeocystis* group is less efficient in iron uptake and more efficient in adapting to low light in the model. The chosen parameter set best matched observed *Phaeocystis* biomass distribution patterns [*Wang and Moore*, 2011].

[8] The light-, nutrient-, and temperature-dependencies of phytoplankton growth rate are modeled multiplicatively. Phytoplankton growth rates decrease under nutrient stress according to Michaelis-Menten nutrients uptake kinetics. Phytoplankton photoadaptation is described by varying

Table 1. Simulation Descriptions

Simulation	AtmCO_2	Forcing	Description
Control	historical	constant climate	provides information about the expected ocean carbon sink with constant climate
Preindustrial	278 ppm	varying climate	provides information about natural carbon storage in the ocean with varying climate
Historical	historical	varying climate	represents the historical scenario (rising CO_2 and varying climate)
Dust	historical	varying climate and dust	provides information about effects of variations in dust deposition

chlorophyll to nitrogen ratios based on the model of *Geider et al.* [1998]. Phytoplankton groups also have variable Fe/C ratios, which vary as a function of ambient iron concentrations. Thus, the BEC model is capable of simulating ocean ecosystem changes under variable mixed layer depths and nutrient supply. Ecosystem parameters were chosen based on field and laboratory data and were described in detail by *Moore et al.* [2002, 2004] and *Wang and Moore* [2011].

[9] The model was spun up for 600 years with repeating National Center for Environmental Prediction/National Center for Atmospheric Research (NCEP/NCAR) meteorological reanalysis climatology data and satellite-based estimates of climatological sea ice cover [*Large and Yeager*, 2004]. The spin-up was long enough so that drifts in upper ocean fluxes decline to negligible levels and the model approached an approximate steady state. The initial distributions of nutrients, inorganic carbon and alkalinity were based on the World Ocean Atlas 2001 database [*Conkright et al.*, 2002] and the GLODAP database [*Key et al.*, 2004]. Dissolved iron initialization was based on simulations from *Moore and Braucher* [2008]. Iron sources in the BEC model included both atmospheric dust deposition and sedimentary diffusion [*Moore and Braucher*, 2008]. Atmospheric CO_2 concentration was set to be 278 ppm for the model initialization. Model year 600 corresponds to the year 1764.

[10] Three different hindcast simulations were performed following the spin-up. Atmospheric CO_2 concentration was held constant at 278 ppm in the first simulation, which represents natural CO_2 flux during the past few decades (preindustrial CO_2 simulation). In the second simulation, reconstructed atmospheric CO_2 concentrations since 1765 were used (referred to as the historical simulation hereafter). This simulation included both natural and anthropogenic variability. In these two simulations, dust deposition was the repeating annual climatology by *Luo et al.* [2003]. The third simulation used the same CO_2 concentrations as the second simulation, and incorporated variable dust deposition since 1948, constrained by observations [*Mahowald et al.*, 2010]. The third simulation focused on variations induced by historical dust changes (referred to as the dust simulation). All three simulations used climatological forcing data until 1947, and the NCEP/NCAR 6-hourly data for momentum, heat, freshwater fluxes and their components since 1948 [*Large and Yeager*, 2009]. Ice fraction satellite data were from the Scanning Multichannel Microwave Radiometer (SMMR) from 1978 to 1988 and Special Sensor Microwave/Imager after 1988 [*Large and Yeager*, 2004]. Climatology data were used when satellite ice fraction data were unavailable, prior to 1978. A control simulation for the estimate of expected CO_2 flux was also performed. The control run was forced with repeating climatological data and the reconstructed, historical atmospheric CO_2 concentrations. Descriptions of the different simulations are summarized in Table 1. The first two simulations and the control simulation are analyzed in section 3.1, in which the trends in fluxes of natural CO_2, anthropogenic CO_2, and total CO_2 are evaluated. The variability of the SO ecosystem is evaluated mainly based on the historical simulation in section 3.2. The impacts of variability in dust deposition are discussed in section 3.3, based on the comparisons between the historical and dust simulations. Significance of trends were calculated with the method of *Santer et al.* [2000] with effective sample sizes considering autocorrelations in the time series. A significance level of 95% was used in this paper. Given trends were significant, except where noted otherwise.

3. Results

[11] Estimates of the sea-air CO_2 flux in the Southern Ocean vary over a wide range, ~ -0.05 PgC/yr to ~ -0.56 PgC/yr for the area below 50°S [*Gloor et al.*, 2003; *Gruber et al.*, 2009; *Gurney et al.*, 2002, 2004; *McNeil et al.*, 2007; *Metzl et al.*, 2006; *Mikaloff Fletcher et al.*, 2006, 2007; *Roy et al.*, 2003; *Takahashi et al.*, 2009; *Wetzel et al.*, 2005]. These studies showed considerable differences and highlight the substantial uncertainty in estimates of sea-air CO_2 flux in the Southern Ocean. The mean contemporary (1994–2003) sea-air CO_2 flux (>50°S) in the historical simulation was 0.06 PgC/yr, on the low end of the range in the previous studies. The simulated CO_2 flux for the area from 14°S to 50°S is -0.95 PgC/yr, similar to the estimate (-1.05 PgC/yr) by *Takahashi et al.* [2009]. The modeled global sea-air CO_2 flux is -1.60 PgC/yr, which is comparable to the estimate of -1.42 PgC/yr given by *Takahashi et al.* [2009] and the estimate of -1.7 PgC/yr by an inversion method by *Gruber et al.* [2009]. Correlations between modeled ΔpCO_2 (atmospheric pCO_2 – surface seawater pCO_2) and estimates by *Takahashi et al.* [2009] are 0.76 globally and 0.54 south of 15°S, respectively.

[12] The BEC model-simulated primary production (>30°S) was 12.4 PgC/yr and annual primary production of the region south of 50°S from 1997 to 2003 was 2.7 PgC/yr, within the range of previous estimates [e.g., *Arrigo et al.*, 1998; *Carr et al.*, 2006; *Moore and Abbott*, 2000]. Global primary production in the BEC model between 1997 and 1998 was 51.7 PgC/yr, comparable with estimates from 24 satellite algorithms (50.7 PgC/yr on average) [*Carr et al.*, 2006]. In our previous study, an observational database of diatoms and *Phaeocystis* biomass in the SO was compiled [*Wang and Moore*, 2011]. A year-by-year comparison is not practical due to the sparseness of observations and difficulties comparing results from a coarse resolution model with field data. However, mean distributions of blooms and the biomass of diatoms and *Phaeocystis* were reasonably captured by the model [*Wang and Moore*, 2011]. The

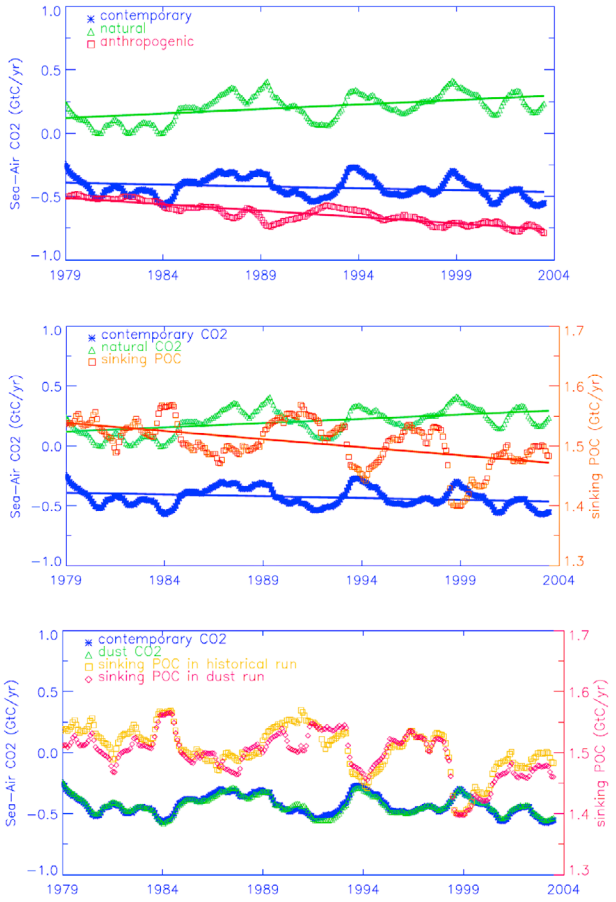

Figure 1. (top) Time series of natural CO_2 flux (green), anthropogenic CO_2 flux (red) and total contemporary CO_2 flux (blue) in the Southern Ocean. (middle) Time series of CO_2 fluxes (green and blue) and sinking POC (marigold). (bottom) Comparison of time series of CO_2 flux and sinking POC in the climatological dust run and historical dust run. Data were smoothed with a 12-month running average.

logarithmic correlation between simulated and observed *Phaeocystis* biomass was 0.67, with a lower value of 0.29 for the diatoms. The logarithmic correlation between simulated annual sinking POC and available sediment trap data is 0.55 over all depths and 0.69 in the upper 1000 m, respectively (n = 46 and 22) (J. K. Moore et al., manuscript in preparation, 2012). The model also did a reasonable job of reproducing observed surface nitrate, phosphate and silicate fields in the Southern Ocean compared with the World Ocean Atlas 2005 (WOA 2005) [*Garcia et al.*, 2006]. The correlation coefficients between simulated surface concentrations of nitrate, phosphate and silicate with WOA 2005 data were all greater than 0.85 [*Wang and Moore*, 2011]. Modeled iron concentrations had a lower correlation with observations from the *Moore and Braucher* [2008] compilation (correlation coefficient of 0.29). However, iron observations are very sparse and do not describe an accurate climatology, as is available for the macronutrients. Detailed evaluation and discussion of the simulated iron field was presented by *Moore and Braucher* [2008].

3.1. Variability in Sea-Air CO_2 Flux and Biological Production

[13] Compared to the expected sea-air CO_2 flux using reconstructed atmospheric CO_2 levels and climatological forcings, a weakening of the SO carbon sink was seen in the historical hindcast simulation. In the pre-industrial CO_2 run, there is a CO_2 outgassing trend of 0.07 PgC/yr/decade between 1948 and 2003 in the region from 40°S to 60°S, which is comparable to the *Wetzel et al.* [2005] result of 0.05 PgC/yr/decade. *Le Quéré et al.* [2007] estimated a weakening trend of 0.08 PgC/yr/decade from 1981 to 2004 below 45°S, compared with 0.06 PgC/yr/decade in this study. Our hindcast simulations produced a similar CO_2 uptake weakening trend in this period of 0.05 PgC/yr/decade below 35°S, corresponding to a decrease of 0.12 PgC/yr in 25 years (Figure 1). Our results agree with these previous studies on the SO CO_2 flux and with the CO_2 flux trend from the study by *Lovenduski et al.* [2007, 2008], which systematically analyzed the long-term trends in CO_2 fluxes and investigated the controlling mechanisms. It was suggested that the weakening SO carbon sink was the combined effect of an increasing anthropogenic carbon sink and a natural CO_2 outgassing. The anthropogenic CO_2 flux closely corresponded to the expected flux under fixed physical forcing, which indicated that the total anthropogenic CO_2 sink remain largely unaltered [*Lovenduski et al.*, 2008]. The natural CO_2 flux also showed a clear trend of increased outgassing in our simulations (Figure 1), caused in part by changes in wind speed [*Lovenduski et al.*, 2008].

[14] The time series of the Southern Ocean export POC sinking at 103 m depth in our simulations had a decreasing trend from 1979 to 2003. This result is different from *Lovenduski et al.* [2007, 2008], who suggested that SO biology changed little and had no significant contribution to the variability in air-sea CO_2 flux. Our simulations showed a decreasing trend in sinking POC of 0.03 PgC/yr/decade from 1979 to 2003, corresponding to a decline of 0.08 PgC/yr in sinking POC flux (Figure 1). Annual primary production declined by 0.4 PgC/yr during this period.

[15] The biological pump has a strong influence on surface pCO_2 and air-sea CO_2 exchange. Variations in sea-air CO_2 flux can mostly be explained by export production changes, under constant climate conditions, as illustrated by *Moore et al.* [2006]. Every 1 PgC of export production led to ~0.6 PgC uptake of atmospheric carbon in their BEC/CCSM3 simulations. The correlation coefficients (r) between the variance in spatially integrated sinking POC and sea-air CO_2 flux were 0.7 in both the natural CO_2 simulation and the contemporary CO_2 simulation. The correlation coefficients between sinking POC anomalies and CO_2 flux anomalies were −0.4 and −0.3, respectively, after the time series were deseasonalized. All correlation coefficients were significant at 95% confidence level. The correlations between sinking POC variance and sea-air CO_2 flux anomalies in the hindcast simulations were much weaker than under constant forcing, because of the significant impacts of variable upwelling and mixing on the solubility pump. But the correlation between the variance in sinking POC and sea-air CO_2 exchange remained significant. About 9% of the variance in CO_2 flux from 1979 to 2003 can be explained by changes in export production.

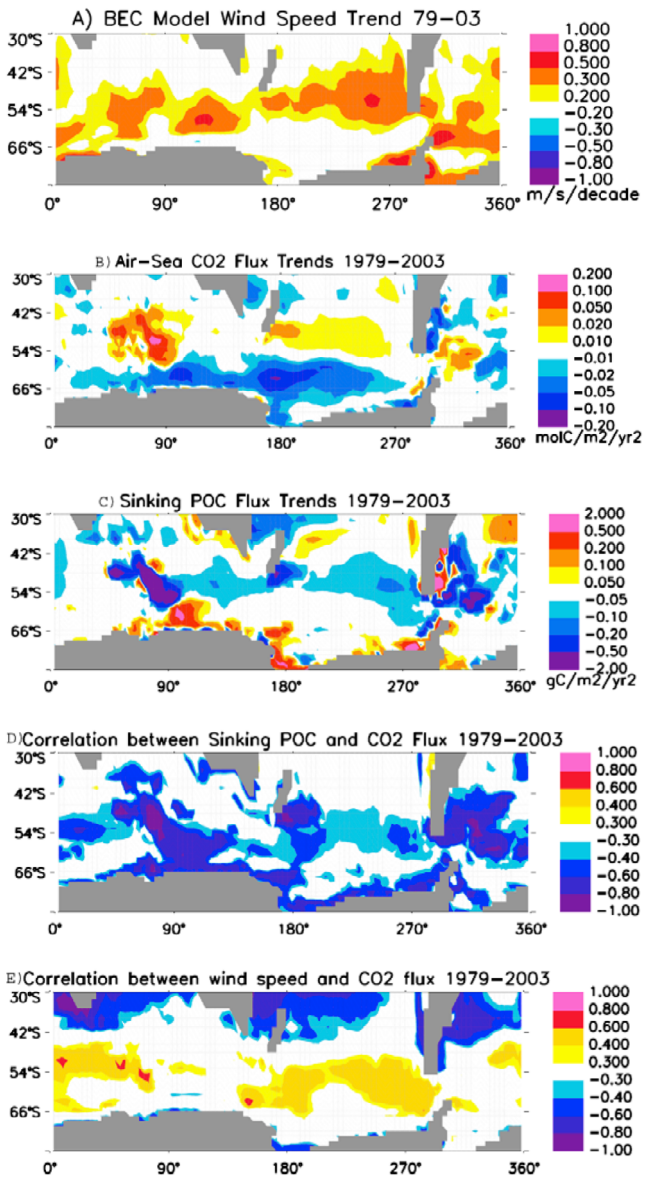

Figure 2. (a) Trends in 10-m wind speed magnitude over the Southern Ocean during 1979 to 2003. (b) Trends in total sea-air CO_2 flux anomalies in the SO in the historical simulation. Positive values indicate a weaker CO_2 uptake or stronger outgassing. (c) Trends in sinking POC anomalies in the same simulation. (d) Correlations between anomalies in sinking POC and sea-air CO_2 flux. (e) Correlations between anomalies in sea-air CO_2 flux and wind speed.

[16] Figure 2 shows a spatial map of trends in monthly sea-air CO_2 flux anomalies and anomalies of biological export production at 103 m from 1979 to 2003. The sea-air CO_2 flux generally exhibited a positive trend from 40°S to 55°S and a negative trend south of 55°S, while sinking POC flux had opposite trends. The spatial map of the correlations between deseasonalized sinking POC and the sea-air CO_2 flux also showed an uneven pattern (Figure 2). In general, the sinking POC can explain most of the variance in the sea-air CO_2 flux in the southernmost regions and suggests a stronger impact of biological production on sea-air CO_2 balance in those regions. The sea-air CO_2 exchange often showed more intensive trends where there were strong trends in sinking POC, such as in the Crozet-Kerguelen and South Georgia regions. It indicates that ocean ecosystems in those regions have experienced significant changes during the study period and those changes have significant impacts on the ocean carbon sink. In contrast, the sea-air CO_2 flux showed increasing carbon uptake in the south Pacific sector between 55°S and 70°S, without any significant change in sinking POC. The variance in biological production and the variance in CO_2 flux are decoupled due to low iron concentrations in the upwelled waters, and biological impacts are weak. This decoupling suggests that the change in the ocean carbon sink in this area was in response to the elevated atmospheric CO_2 levels and changing physical circulation and mixing.

[17] The spatial trends of primary production varied between phytoplankton functional groups (Figure 3). Phytoplankton groups showed opposite trends in some regions, resulting in no significant trend in total primary production. Primary production exhibited a general increasing trend south of 60°S, which was contributed mainly by the larger phytoplankton groups. Decreased small phytoplankton production led to a strong declining trend in primary production between 40°S–60°S. In the BEC model, phytoplankton

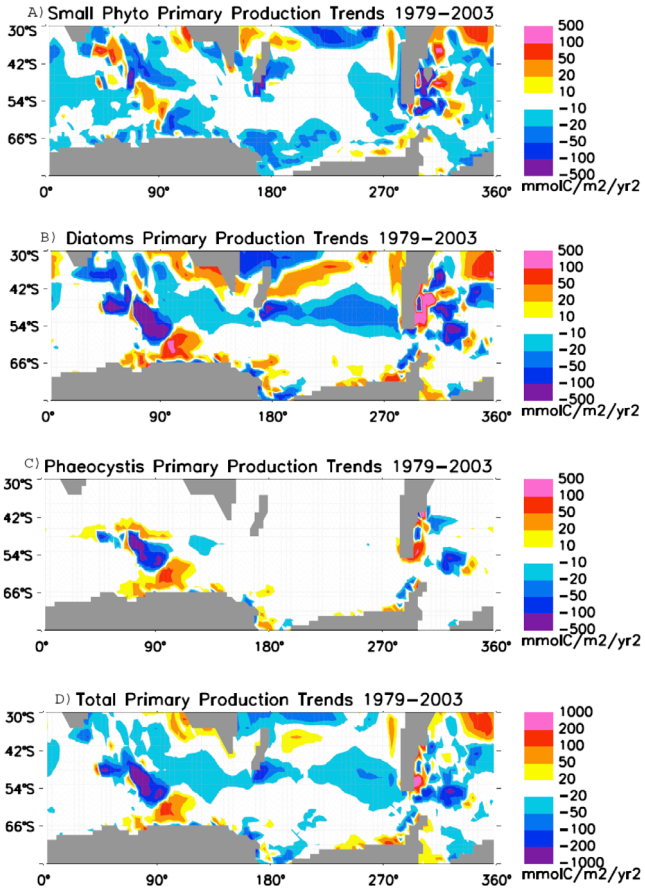

Figure 3. Trends in primary production anomalies in the SO during 1979 to 2003 in the historical simulation of (a) the small phytoplankton group, (b) diatoms, (c) *Phaeocystis* and (d) total primary production.

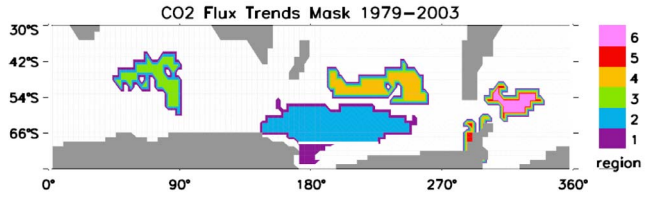

Figure 4. Highlighted are regions where there were strong trends in sea-air CO_2 flux during 1979 to 2003 in the historical simulation. They are the western Ross Sea, the high latitude Pacific (55°S–70°S), Crozet-Kerguelen, the midlatitude Pacific (40°S–55°S), the west Antarctic Peninsula and South Georgia.

groups have different favorable conditions for growth, and the larger phytoplankton export organic matter more efficiently, which can decrease primary production, even as export production is increasing. The diverse patterns in production variability imply that the controls on phytoplankton growth are complicated and not uniform over the Southern Ocean. The mechanisms which may influence the ocean solubility pump have been discussed in detail in a previous study [*Lovenduski et al.*, 2008]. Here we focus on several distinct regions in the SO where there were significant changes in the ocean carbon sink or biological productivity, to investigate trends in the ecosystem and the biological pump, as well as the different mechanisms which may drive those trends.

3.2. Factors Driving Variability

[18] To diagnose the driving mechanisms, we identify several regions where there are clear trends in sea-air CO_2 flux (Figures 2b and 4). These regions are displayed in Figure 4 and include Crozet-Kerguelen (Figure 5a), South Georgia (Figure 5b), midlatitude Pacific (40°S–55°S, Figure 5c), high latitude Pacific (55°S–70°S, Figure 5d), western Antarctic Peninsula (Figure 5e) and the western Ross Sea (Figure 5f). Since the biological pump has the largest impacts during austral summer, we examined the time series of sea-air CO_2 flux, sinking POC, primary production, and physical fields in the summer season (December–February). PAR averaged over mixed layer and surface nutrient concentration time series are plotted for November, which indicate early spring conditions for phytoplankton growth, and play a key role in determining the total summertime production. Time series of ice fraction in December are also included for western Antarctic Peninsula (Figure 5e) and the western Ross Sea (Figure 5f). We examined the growth limiting factors for each phytoplankton functional group from November to February. Regional trends and driving mechanisms are summarized in Table 2.

[19] The Crozet Plateau and Kerguelen Plateau are major bathymetric features with islands on the pathway of the eastward-flowing ACC. The bathymetry at these plateaus influences circulation pathways and transport, and leads to iron-enriched surface waters [*Mongin et al.*, 2009; *Park et al.*, 2008; *Pollard et al.*, 2007]. Large phytoplankton blooms were induced by natural iron-fertilization in this region, impacting the ocean carbon sink [*Blain et al.*, 2007; *Jouandet et al.*, 2008]. Our simulations show a strong decreasing trend of ocean CO_2 uptake (0.14 mol/m^2/decade carbon, in Figure 5a and Table 2). During the same period, there was a significant decrease in phytoplankton production (−0.53 mol/m^2/decade carbon). The correlation coefficient between sea-air CO_2 exchange and sinking POC is high at −0.97. The growth of phytoplankton in the Crozet-Kerguelen region is relatively less nutrient-stressed and more light-limited due to the supply of iron and major nutrients brought to the surface by mixing. The growth of small phytoplankton during the summer season is generally limited by light, while diatoms and *Phaeocystis* groups are co-limited by both ambient iron concentrations and light [*Wang and Moore*, 2011]. Thus, phytoplankton production is quite sensitive to light availability in this region, where there is a strong sedimentary iron source. All the phytoplankton groups experienced an increasing light limitation over this period due to the decline of mean PAR, in the deepening mixed layer (Figure 5a). Iron concentrations in the mixed layer in spring had no significant trend. Note that the large sea-air CO_2 flux trend was greatly modified by the unusually strong ocean carbon sink around 1983–1984, which coincided with an ENSO event, though this concurrence did not hold over the whole period.

[20] The South Georgia region, in the South Atlantic, is another location where iron from the island or surrounding shallow plateau fertilizes the mixed layer and induces blooms, when light levels are high enough for growth [*Kahru et al.*, 2007; *Moore and Abbott*, 2000; *Moore et al.*, 2002; *Ward et al.*, 2007]. Ocean carbon uptake in summer weakened at a rate of 0.10 mol/m^2/decade during 1979 to 2003, but was not statistically significant (Figure 5b and Table 2). The summer POC sinking flux shows a decreasing trend of 0.19 mol/m^2/decade. The correlation coefficient between summer sea-air CO_2 flux and sinking POC was −0.94 over the study period. This region had shallower mixed layer depths than the Crozet-Kerguelen region at the beginning of the study period. Except for the small phytoplankton, the phytoplankton groups were more iron limited. Simulations showed a significant increase in mixed layer depths and decrease in PAR, which caused the most limiting factor for the diatom group to switch to light limitation (Figure 5b). Diatoms are the dominant phytoplankton in this region [*Korb et al.*, 2008]. The trend in light availability drives the decreasing trend in phytoplankton growth and production in South Georgia region. The Crozet Plateau, Kerguelen Plateau and South Georgia are all high nutrient, high chlorophyll regions within the SO. Phytoplankton production showed similar trends in these regions and the difference in trends of sinking POC was a result of changes in phytoplankton community and bloom magnitudes.

[21] During the summer season, trends in the biological pump and sea-air CO_2 flux are weaker in the midlatitude (40°S–55°S) Pacific region, as is the correlation between the biological pump and sea-air CO_2 flux (Figure 5c and Table 2). The magnitude of changes in sinking POC is approximately half of the magnitude in sea-air CO_2 flux variations, which indicates that the variations in biological pump play a less important role. Phytoplankton growth was limited by low ambient iron concentrations. The deepening mixed layer leads to moderately increased light limitation and a total decline of 0.13 mol/m^2 in summer primary production during 1979 to 2003. Increased CO_2

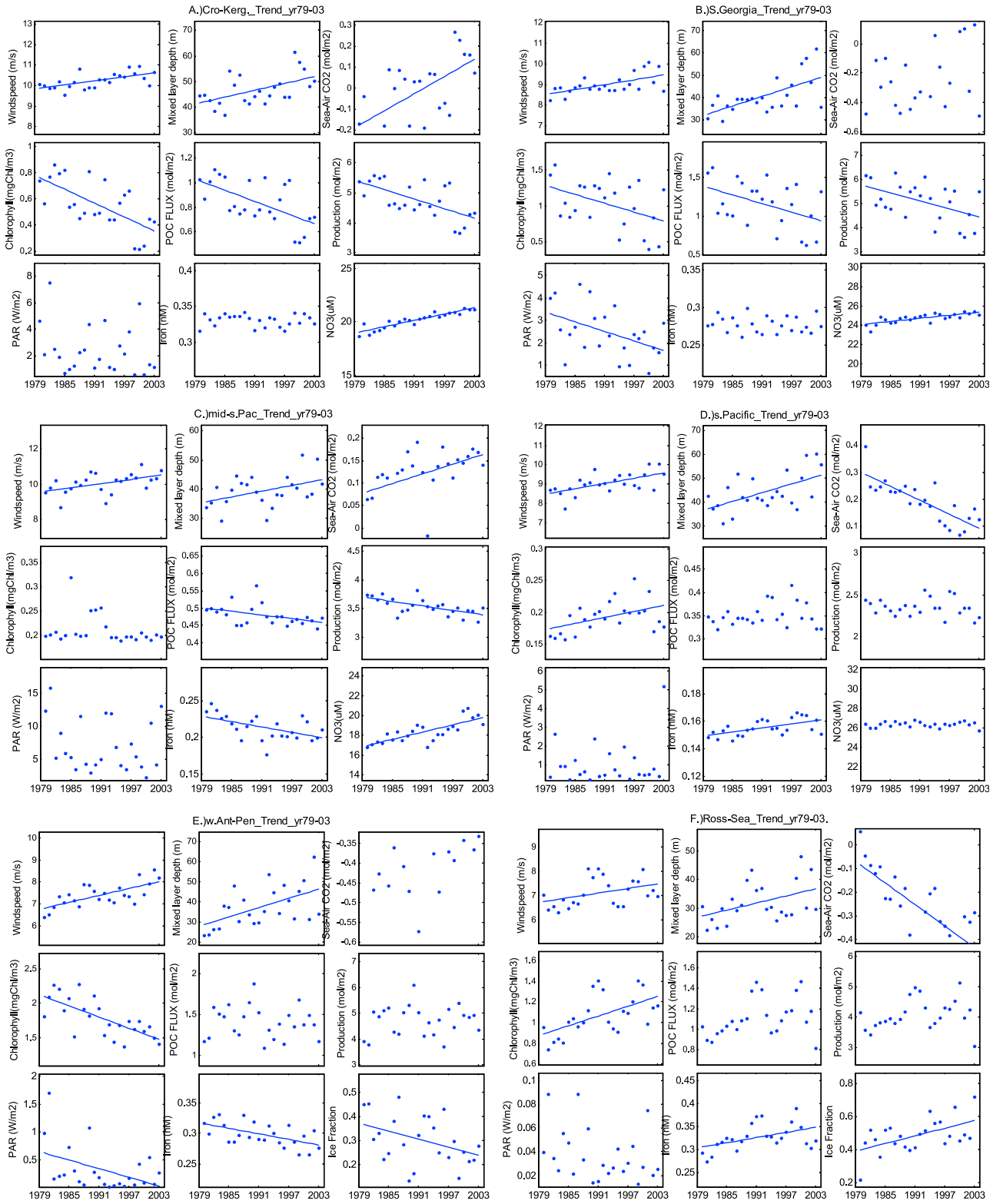

Figure 5. Time series are shown for regions in the Southern Ocean (marked in Figure 4). Shown are (a) Crozet-Kerguelen, (b) South Georgia, (c) midlatitude Pacific, (d) high latitude Pacific, (e) western Antarctic Peninsula, and (f) western Ross Sea. Data for wind speed, mixed layer depth and surface chlorophyll were summer season means (December, January, and February). Data for sea-air CO_2 flux, sinking POC and primary production were summed over summer months. PAR and nutrient concentrations (iron and nitrogen) were from November, in austral spring. Time series of ice fraction in December were included for Figures 5e and 5f. Only significant trend lines (≥95%) are plotted.

Table 2. Summary of Regional Trends and Driving Factors

Region	CO_2 Flux Trend (mol/m^2/decade)	Correlation With POC Flux	Major Controls on CO_2 Flux
Crozet-Kerguelen	0.14	−0.97	The trend was mainly driven by biological pump.
South Georgia	not significant	−0.94	Variability is largely explained by the biological pump, but there was no significant trend in CO_2 flux.
Midlatitude Pacific	0.04	not significant	The increased CO_2 outgassing was mainly driven by stronger winds and upwelling.
High latitude Pacific	−0.09	not significant	The trend in CO_2 flux was dominated by the increase in anthropogenic CO_2 uptake.
Western Antarctic Peninsula	not significant	−0.77	Variability was largely explained by the biological pump, but there was no significant CO_2 flux trend.
Western Ross Sea	−0.15	−0.81	The trend was mainly driven by the biological pump.

outgassing was mainly driven by stronger winds and upwelling (as suggested by *Lovenduski et al.* [2008]).

[22] The high latitude Pacific (55°S–70°S) is a typical High Nutrient, Low Chlorophyll (HNLC) region, and a decreasing source for atmospheric CO_2 (Figure 5d). Phytoplankton growth was limited by iron. From 1979 to 2003, ambient iron concentrations increased a little, which led to a slight increase in sinking POC. The trend is dominated by a small area near the Antarctic continent, where phytoplankton productivity is higher than other parts of this region due to continental iron supply. The overall trend in summer sinking POC was not statistically significant (Figure 5d), and there was no significant correlation between sinking POC and sea-air CO_2 flux over most of this region (Figure 2). This suggests that the trend in sea-air CO_2 balance is dominated by the solubility pump. The increasing trend in CO_2 ocean uptake was dominated by the significant increase in anthropogenic CO_2 uptake in agreement with previous studies [*Ito et al.*, 2010; *Lovenduski et al.*, 2008].

[23] Previous studies showed clear changes in chlorophyll concentrations and ecosystem communities in the western Antarctic Peninsula region with climate change, such as changes in sea-ice coverage and the SAM [*Montes-Hugo et al.*, 2009, 2008; *Stammerjohn et al.*, 2008; *Vernet et al.*, 2008]. Our simulation had a significant decrease in summertime surface chlorophyll from 1979 to 2003. There was a small ∼1% decrease in primary production over the study period. Our result agrees with previous studies, which found no significant trend in primary production along the western Antarctic Peninsula [*Vernet et al.*, 2008], but a decrease in summertime surface chlorophyll over the past three decades [*Montes-Hugo et al.*, 2009]. Though there was no significant change in total primary production, opposite trends in small phytoplankton production and large phytoplankton production, especially diatoms, were produced in the simulation (Figure 3), because deepened mixed layers increased light stress for phytoplankton. Spring iron concentrations also declined. The trend in sea-air CO_2 flux was relatively small, but the variation was negatively correlated with sinking POC (correlation coefficient −0.77). Figure 5e shows the December ice fraction in this region. Years with higher spring ice fractions exhibited lower summertime primary production. Interannual variability of sinking POC and primary production showed strong correlations with spring ice fraction and mixed layer depth. This indicates that interannual variability in phytoplankton community is largely regulated by mixed layer depth, spring sea ice retreat and circulation, as noted in previous work [*Garibotti et al.*, 2005; *Montes-Hugo et al.*, 2008; *Smith et al.*, 2008; *Stammerjohn et al.*, 2008].

[24] The Ross Sea region had an increasing trend of 0.15 mol/m^2/decade in summertime ocean carbon uptake and a concurrent increasing trend of 0.09 mol/m^2/decade in POC export. Though the contribution of the biological pump to total sea-air CO_2 exchange is smaller in the Ross Sea than in the Crozet-Kerguelen and the South Georgia regions, the interannual CO_2 flux was well correlated with biological production (Figure 5f and Table 2). The variability in primary production in the Ross Sea region was well correlated with wind speed variations, which control mixed layer depths. As the mixed layer deepened, sinking POC and primary production increased in this region. This is because the most limiting factor for the summertime growth is ambient iron availability in this region for all phytoplankton groups in the model. Stronger vertical mixing brings up more iron, which results in higher phytoplankton production. This particularly strong correlation between wind speed and primary production was also noted previously [*Arrigo et al.*, 2008]. Changes in sea ice cover also played an important role in the interannual variability in POC and CO_2 fluxes, since ice coverage has strong impacts on irradiance, which affect the onsets of blooms [*Smith and Comiso*, 2008]. For example, heavy sea ice cover in 2002 and 2003 led to a strong decrease in primary production and a decline in ocean carbon uptake, as found in previous satellite studies [*Arrigo and Van Dijken*, 2007]. Mixed layer depths, though increasing, remained relatively shallow with little impact on PAR (Figure 5f).

[25] The sea-air CO_2 flux exhibited distinct patterns in different regions of the SO. Despite the important role of the solubility pump, sea-air CO_2 flux trends were largely attributed to phytoplankton production variability, especially in bloom regions, near islands, plateaus and along the continental shelves. Variability in primary production and sinking POC is tightly linked to variations in nutrient availability and the light regime. Around islands and plateaus, trends in phytoplankton production were mainly driven by light availability, because light often limits phytoplankton growth more in these iron-enriched waters, in part due to self-shading at higher chlorophyll concentrations [*de Baar et al.*, 2005; *Krishnamurthy et al.*, 2008]. Iron concentration change was the major driver for production trends in the open ocean, which depends on local mixing processes, atmospheric deposition, and lateral transport. Besides changes in mixed layer depths and iron concentrations, productivity near Antarctica was also influenced by

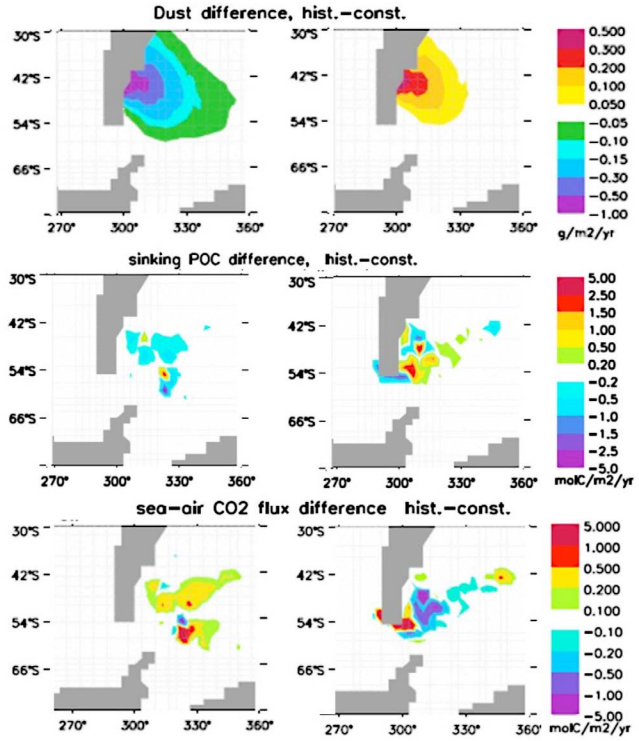

Figure 6. Differences in (top) dust deposition, (middle) sinking POC and (bottom) sea-air CO_2 flux between simulations with historical varying dust and climatological dust deposition are shown (left, low-dust year; right, high-dust year).

sea ice cover. Satellite-observed sea ice fractions were used as a boundary condition for calculations of gas exchange and PAR, but the full effects of sea ice on circulation were not included in these simulations. Fully coupled ocean-ice simulations could better examine the influence of sea ice.

[26] Contrary to the finding by *Lovenduski et al.* [2008], significant interannual and decadal variations of the SO phytoplankton community composition and production were found in this study. There are several factors likely causing these differences. Simulated mixed layer depths in the SO are more realistic in this study. As discussed above, productivity can be very sensitive to changes in mean irradiance in the mixed layer. The improved (deeper) mixed layer depths in our simulations allow the BEC model to better capture the light limitation for phytoplankton growth due to mixed layer deepening. Second, an improved iron cycle with better scavenging parameterizations and a realistic sedimentary iron source, based on a large, global data set of observations, is used in this study [*Moore and Braucher*, 2008]. There is no doubt that ambient iron concentrations are crucial for determining productivity in the Southern Ocean, which is the largest HNLC region and where productivity is often limited by iron. Third, the current BEC model includes an additional phytoplankton functional group, *Phaeocystis*, which is known to be an important phytoplankton species in the SO [e.g., *Mathot et al.*, 2000; *Poulton et al.*, 2007]. This provides a more realistic ecosystem and perhaps allows the model to better capture variability in phytoplankton community structure and primary production.

3.3. Dust-Driven Variability in Production and CO_2 Flux

[27] The spatially integrated CO_2 flux time series in the dust simulation and the constant dust simulation were almost identical (Figure 1). This indicates that the variability in dust deposition to the Southern Ocean during the study period was not large enough to induce large changes in integrated CO_2 flux. There was also no significant difference in global integrated ocean carbon uptake in simulations with constant dust and historical dust. A previous modeling study produced CO_2 flux anomalies of ~0.2 PgC/yr globally, induced by dust deposition variations, and suggested changes in dust deposition may also be a cause of the decreasing trend of ocean carbon sink in the Southern Ocean [*Doney et al.*, 2009a]. There are two reasons for this discrepancy. The reconstructed dust deposition used in our simulations was constrained by observations in our simulation [*Mahowald et al.*, 2010]; while an earlier model-produced dust deposition was used in the previous study. That dust model may overestimate the importance of dust deposition to the SO [*Wagener et al.*, 2008]. Second, the BEC model used in our simulation employs the modified iron cycle, which has a stronger sedimentary iron source, and thus is less sensitive to variations in atmospheric dust deposition [*Moore and Braucher*, 2008]. However, there are some differences in sinking POC, caused by the variability in iron supply from dust deposition, which can be important regionally, and potentially decouple biological production, sinking POC and sea-air CO_2 flux from physical processes in the ocean.

[28] Dust deposition over the SO mainly falls in regions downwind of dust sources, near Australia, south of Africa, and southwest of South America. There were higher dust fluxes to the SO during the late 1980s and early 1990s and less dust deposition in the early 80s and later in the 1990s. Areas downwind of South America and Australia experienced the largest variations in dust deposition. Ocean biology is most sensitive to dust variations near South America in the BEC model. The biological response was much smaller south of Australia. This agrees with *Mackie et al.* [2008], who found no iron-mediated algal blooms during the largest Australian dust storms in the past 40 years. The interannual variability in total dust deposition over the SO is generally less than 10%. Here we select two distinct years with high dust deposition and low dust deposition, respectively, to examine the influence of dust deposition on the ocean carbon sink and biological production near the South America dust source region. Figure 6 shows the differences in dust deposition, sinking POC and CO_2 flux, downwind of South America, between the varying and constant dust simulations. Since changing dust deposition has no impact on physical fields, all differences are due to the deposition. When dust deposition was about 10% lower than climatological deposition (Figure 6, left), sinking POC was 0.08 molC/m^2/yr less and the ocean carbon sink was 0.07 molC/m^2/yr lower. When dust deposition was about 5% higher than climatological deposition (Figure 6, right), sinking POC increased by 0.10 molC/m^2/yr and CO_2 uptake increased by 0.11 molC/m^2/yr. Thus,

variations in dust deposition can alter regional patterns of biological production and the ocean carbon sink.

4. Summary

[29] A weakening trend in SO carbon uptake was found based on a series of hindcast simulations, similar to some previous work [*Le Quéré et al.*, 2007; *Lovenduski et al.*, 2007; *Wetzel et al.*, 2005]. Our simulations showed significant impacts of the biological pump on the SO carbon sink. The results showed decreasing trends in primary production and sinking POC from 1979 to 2003. The driving mechanisms of these trends varied between regions. Growth limitations by the irradiance regime and iron concentrations largely drive the variability in productivity. Variations in atmospheric dust deposition can affect productivity and sea-air CO_2 flux in areas downwind of dust source regions, but have little influence on total SO productivity and the carbon sink.

[30] The investigation of long-term trends in the global carbon cycle requires a comprehensive understanding of the impacts of interannual varying forcing on air-sea CO_2 flux and phytoplankton productivity in the SO. Our results suggest that SO phytoplankton productivity is sensitive to climate change and has significant impacts on the SO carbon cycle, especially in high-productivity regions. A number of previous studies have suggested that iron-light co-limitation is common in the Southern Ocean [*Boyd et al.*, 1999, 2001; *Boyd*, 2002; *de Baar et al.*, 2005; *Krishnamurthy et al.*, 2008]. However, coarse resolution circulation models tend to underestimate mixed layer depths in this region, potentially missing a key control on biological productivity.

[31] One major caveat in this work is that the coarse resolution model cannot resolve eddy dynamics. Recent work suggested that eddies are important in controlling the response of circulation to changes in wind stress [*Böning et al.*, 2008]. The crucial role of eddies was also highlighted in a recent study of anthropogenic CO_2 transport, since the Ekman-driven transport and eddy-driven transport oppose each other [*Ito et al.*, 2010]. Eddies also affect the transport of nutrients. Future simulations in coupled, eddy-permitting models could help clarify the role of eddies in the circulation and their impacts on biogeochemistry in a changing climate.

[32] This study emphasizes the important role of the biological pump in the SO carbon cycle in the context of a changing climate. Considerable uncertainties remain concerning the mechanisms driving primary production variability and the impacts of ecosystem dynamics on air-sea CO_2 exchange. It is necessary to further develop both physical and ecosystem models to better capture the dynamics of ocean ecosystems, and to study the biological impacts on the carbon cycle under past and future climate scenarios.

[33] **Acknowledgments.** This work was supported by funding from NASA grants NNG05GR25G and NNX08AB76G to J. K. Moore. Computations were supported by the Earth System Modeling Facility at UCI (NSF ATM-O321380). Thanks to I. Lima and K. Lindsay for support in model simulations used in this study. We also thank N. Lovenduski for helpful conversations and suggestions in simulation analysis.

References

Archer, C. L., and K. Caldeira (2008), Historical trends in the jet streams, *Geophys. Res. Lett.*, *35*, L08803, doi:10.1029/2008GL033614.

Arrigo, K. R., and G. L. Van Dijken (2007), Interannual variation in air-sea CO_2 flux in the Ross Sea, Antarctica: A model analysis, *J. Geophys. Res.*, *112*, C03020, doi:10.1029/2006JC003492.

Arrigo, K. R., D. Worthen, A. Schnell, and M. P. Lizotte (1998), Primary production in Southern Ocean waters, *J. Geophys. Res.*, *103*(C8), 15,587–15,600, doi:10.1029/98JC00930.

Arrigo, K. R., G. L. van Dijken, and S. Bushinsky (2008), Primary production in the Southern Ocean, 1997–2006, *J. Geophys. Res.*, *113*, C08004, doi:10.1029/2007JC004551.

Behrenfeld, M. J., R. T. O'Malley, D. A. Siegel, C. R. McClain, J. L. Sarmiento, G. C. Feldman, A. J. Milligan, P. G. Falkowski, R. M. Letelier, and E. S. Boss (2006), Climate-driven trends in contemporary ocean productivity, *Nature*, *444*(7120), 752–755, doi:10.1038/nature05317.

Biastoch, A., C. W. Boning, F. U. Schwarzkopf, and J. R. E. Lutjeharms (2009), Increase in Agulhas leakage due to poleward shift of Southern Hemisphere westerlies, *Nature*, *462*(7272), 495–498, doi:10.1038/nature08519.

Blain, S., et al. (2007), Effect of natural iron fertilization on carbon sequestration in the Southern Ocean, *Nature*, *446*(7139), 1070–1074, doi:10.1038/nature05700.

Böning, C. W., A. Dispert, M. Visbeck, S. R. Rintoul, and F. U. Schwarzkopf (2008), The response of the Antarctic Circumpolar Current to recent climate change, *Nat. Geosci.*, *1*(12), 864–869, doi:10.1038/ngeo362.

Boyd, P. W. (2002), Environmental factors controlling phytoplankton processes in the Southern Ocean, *J. Phycol.*, *38*(5), 844–861, doi:10.1046/j.1529-8817.2002.t01-1-01203.x.

Boyd, P. W., J. LaRoche, M. Gall, R. Frew, and R. M. L. McKay (1999), Role of iron, light, and silicate in controlling algal biomass in subantarctic waters SE of New Zealand, *J. Geophys. Res.*, *104*(C6), 13,395–13,408, doi:10.1029/1999JC900009.

Boyd, P. W., A. C. Crossley, G. R. DiTullio, F. B. Griffiths, D. A. Hutchins, B. Queguiner, P. N. Sedwick, and T. W. Trull (2001), Control of phytoplankton growth by iron supply and irradiance in the subantarctic Southern Ocean: Experimental results from the SAZ Project, *J. Geophys. Res.*, *106*(C12), 31,573–31,583, doi:10.1029/2000JC000348.

Brierley, A. S., and M. J. Kingsford (2009), Impacts of climate change on marine organisms and ecosystems, *Curr. Biol.*, *19*(14), R602–R614, doi:10.1016/j.cub.2009.05.046

Cai, W. (2006), Antarctic ozone depletion causes an intensification of the Southern Ocean super-gyre circulation, *Geophys. Res. Lett.*, *33*, L03712, doi:10.1029/2005GL024911.

Carr, M.-E., et al. (2006), A comparison of global estimates of marine primary production from ocean color, *Deep Sea Res., Part II*, *53*(5–7), 741–770, doi:10.1016/j.dsr2.2006.01.028.

Cassar, N., M. L. Bender, B. A. Barnett, S. Fan, W. J. Moxim, H. Levy II, and B. Tilbrook (2007), The Southern Ocean biological response to aeolian iron deposition, *Science*, *317*(5841), 1067–1070, doi:10.1126/science.1144602.

Collins, W. D., et al. (2006), The Community Climate System Model Version 3(CCSM3), *J. Clim.*, *19*(11), 2122–2143, doi:10.1175/JCLI3761.1.

Comiso, J. C. (2000), Variability and trends in Antarctic surface temperatures from in situ and satellite infrared measurements, *J. Clim.*, *13*(10), 1674–1696, doi:10.1175/1520-0442(2000)013<1674:VATIAS>2.0.CO;2.

Comiso, J. C., and F. Nishio (2008), Trends in the sea ice cover using enhanced and compatible AMSR-E, SSM/I, and SMMR data, *J. Geophys. Res.*, *113*, C02S07, doi:10.1029/2007JC004257.

Conkright, M. E., R. A. Locarnini, H. E. Garcia, T. D. O'Brien, T. P. Boyer, C. Stephens, and J. J. Antonov (2002), *World Ocean Atlas 2001: Objective Analysis, Data Statistics, and Figures, CDROM Documentation*, 17 pp., Ocean Clim. Lab., Natl. Oceanogr. Data Cent., Silver Spring, Md.

de Baar, H. J. W., et al. (2005), Synthesis of iron fertilization experiments: From the Iron Age in the Age of Enlightenment, *J. Geophys. Res.*, *110*, C09S16, doi:10.1029/2004JC002601.

de Boyer Montégut, C., G. Madec, A. S. Fischer, A. Lazar, and D. Iudicone (2004), Mixed layer depth over the global ocean: An examination of profile data and a profile-based climatology, *J. Geophys. Res.*, *109*, C12003, doi:10.1029/2004JC002378.

DiTullio, G. R., J. M. Grebmeier, K. R. Arrigo, M. P. Lizotte, D. H. Robinson, A. Leventer, J. P. Barry, M. L. VanWoert, and R. B. Dunbar (2000), Rapid and early export of *Phaeocystis antarctica* blooms in the Ross Sea, Antarctica, *Nature*, *404*(6778), 595–598, doi:10.1038/35007061.

Doney, S. C., I. Lima, R. A. Feely, D. M. Glover, K. Lindsay, N. Mahowald, J. K. Moore, and R. Wanninkhof (2009a), Mechanisms governing interannual variability in upper-ocean inorganic carbon system and air-sea CO_2 fluxes: Physical climate and atmospheric dust, *Deep Sea Res., Part II*, *56*(8–10), 640–655, doi:10.1016/j.dsr2.2008.12.006.

Doney, S. C., I. Lima, J. K. Moore, K. Lindsay, M. J. Behrenfeld, T. K. Westberry, N. Mahowald, D. M. Glover, and T. Takahashi (2009b), Skill metrics for confronting global upper ocean ecosystem-biogeochemistry models against field and remote sensing data, *J. Mar. Syst.*, *76*(1–2), 95–112, doi:10.1016/j.jmarsys.2008.05.015.

Feng, Y., et al. (2010), Interactive effects of iron, irradiance and CO_2 on Ross Sea phytoplankton, *Deep Sea Res., Part I*, *57*(3), 368–383, doi:10.1016/j.dsr.2009.10.013.

Gabric, A. J., R. A. Cropp, G. H. McTainsh, B. M. Johnston, H. Butler, B. Tilbrook, and M. Keywood (2010), Australian dust storms in 2002–2003 and their impact on Southern Ocean biogeochemistry, *Global Biogeochem. Cycles*, *24*, GB2005, doi:10.1029/2009GB003541.

Garcia, H. E., R. A. Locarnini, T. P. Boyer, and J. I. Antonov (2006), *World Ocean Atlas 2005*, vol. 4, *Nutrients (Phosphate, Nitrate, Silicate), NOAA Atlas NESDIS 64*, edited by S. Levitus, 396 pp., NOAA, Silver Spring, Md.

Garibotti, I. A., M. Vernet, R. C. Smith, and M. E. Ferrario (2005), Interannual variability in the distribution of the phytoplankton standing stock across the seasonal sea-ice zone west of the Antarctic Peninsula, *J. Plankton Res.*, *27*(8), 825–843, doi:10.1093/plankt/fbi056.

Geider, R. J., H. L. MacIntyre, and T. M. Kana (1998), A dynamic regulatory model of phytoplanktonic acclimation to light, nutrients, and temperature, *Limnol. Oceanogr.*, *43*(4), 679–694, doi:10.4319/lo.1998.43.4.0679.

Gille, S. T. (2008), Decadal-scale temperature trends in the Southern Hemisphere ocean, *J. Clim.*, *21*(18), 4749–4765, doi:10.1175/2008JCLI2131.1.

Gloor, M., N. Gruber, J. Sarmiento, C. L. Sabine, R. A. Feely, and C. Rödenbeck (2003), A first estimate of present and preindustrial air-sea CO_2 flux patterns based on ocean interior carbon measurements and models, *Geophys. Res. Lett.*, *30*(1), 1010, doi:10.1029/2002GL015594.

Gruber, N., et al. (2009), Oceanic sources, sinks, and transport of atmospheric CO_2, *Global Biogeochem. Cycles*, *23*, GB1005, doi:10.1029/2008GB003349.

Gurney, K. R., et al. (2002), Towards robust regional estimates of CO_2 sources and sinks using atmospheric transport models, *Nature*, *415*(6872), 626–630, doi:10.1038/415626a.

Gurney, K. R., et al. (2004), Transcom 3 inversion intercomparison: Model mean results for the estimation of seasonal carbon sources and sinks, *Global Biogeochem. Cycles*, *18*, GB1010, doi:10.1029/2003GB002111.

Ito, T., M. Woloszyn, and M. Mazloff (2010), Anthropogenic carbon dioxide transport in the Southern Ocean driven by Ekman flow, *Nature*, *463*(7277), 80–83, doi:10.1038/nature08687.

Jouandet, M. P., S. Blain, N. Metzl, C. Brunet, T. W. Trull, and I. Obernosterer (2008), A seasonal carbon budget for a naturally iron-fertilized bloom over the Kerguelen Plateau in the Southern Ocean, *Deep Sea Res., Part II*, *55*(5–7), 856–867, doi:10.1016/j.dsr2.2007.12.037.

Kahru, M., B. G. Mitchell, S. T. Gille, C. D. Hewes, and O. Holm-Hansen (2007), Eddies enhance biological production in the Weddell-Scotia Confluence of the Southern Ocean, *Geophys. Res. Lett.*, *34*, L14603, doi:10.1029/2007GL030430.

Key, R. M., A. Kozyr, C. L. Sabine, K. Lee, R. Wanninkhof, J. L. Bullister, R. A. Feely, F. J. Millero, C. Mordy, and T. H. Peng (2004), A global ocean carbon climatology: Results from Global Data Analysis Project (GLODAP), *Global Biogeochem. Cycles*, *18*, GB4031, doi:10.1029/2004GB002247.

Khatiwala, S., F. Primeau, and T. Hall (2009), Reconstruction of the history of anthropogenic CO_2 concentrations in the ocean, *Nature*, *462*(7271), 346–349, doi:10.1038/nature08526.

Korb, R. E., M. J. Whitehouse, A. Atkinson, and S. E. Thorpe (2008), Magnitude and maintenance of the phytoplankton bloom at South Georgia: A naturally iron-replete environment, *Mar. Ecol. Prog. Ser.*, *368*, 75–91, doi:10.3354/meps07525.

Krishnamurthy, A., J. K. Moore, and S. C. Doney (2008), The effects of dilution and mixed layer depth on deliberate ocean iron fertilization: 1-D simulations of the southern ocean iron experiment (SOFeX), *J. Mar. Syst.*, *71*(1–2), 112–130, doi:10.1016/j.jmarsys.2007.07.002.

Large, W. G., and S. G. Yeager (2004), Diurnal to decadal global forcing for ocean and sea-ice models: The data sets and flux climatologies, *NCAR Tech. Note, NCAR/TN-460+STR*, 105 pp., Natl. Cent. for Atmos. Res., Boulder, Colo.

Large, W. G., and S. G. Yeager (2009), The global climatology of an interannually varying air–sea flux data set, *Clim. Dyn.*, *33*(2), 341–364, doi:10.1007/s00382-008-0441-3.

Law, R. M., R. J. Matear, and R. J. Francey (2008), Comment on "Saturation of the Southern Ocean CO_2 sink due to recent climate change," *Science*, *319*(5863), 570a, doi:10.1126/science.1149077.

Le Quéré, C., et al. (2007), Saturation of the Southern Ocean CO_2 sink due to recent climate change, *Science*, *316*(5832), 1735–1738, doi:10.1126/science.1136188.

Lovenduski, N. S., N. Gruber, S. C. Doney, and I. D. Lima (2007), Enhanced CO_2 outgassing in the Southern Ocean from a positive phase of the Southern Annular Mode, *Global Biogeochem. Cycles*, *21*, GB2026, doi:10.1029/2006GB002900.

Lovenduski, N. S., N. Gruber, and S. C. Doney (2008), Toward a mechanistic understanding of the decadal trends in the Southern Ocean carbon sink, *Global Biogeochem. Cycles*, *22*, GB3016, doi:10.1029/2007GB003139.

Luo, C., N. M. Mahowald, and J. del Corral (2003), Sensitivity study of meteorological parameters on mineral aerosol mobilization, transport, and distribution, *J. Geophys. Res.*, *108*(D15), 4447, doi:10.1029/2003JD003483.

Mackie, D. S., P. W. Boyd, G. H. McTainsh, N. W. Tindale, T. K. Westberry, and K. A. Hunter (2008), Biogeochemistry of iron in Australian dust: From eolian uplift to marine uptake, *Geochem. Geophys. Geosyst.*, *9*, Q03Q08, doi:10.1029/2007GC001813.

Mahowald, N. M., et al. (2010), Observed 20th century desert dust variability: Impact on climate and biogeochemistry, *Atmos. Chem. Phys.*, *10*(22), 10,875–10,893, doi:10.5194/acp-10-10875-2010.

Marinov, I., A. Gnanadesikan, J. R. Toggweiler, and J. L. Sarmiento (2006), The Southern Ocean biogeochemical divide, *Nature*, *441*(7096), 964–967, doi:10.1038/nature04883.

Matear, R. J., and A. Lenton (2008), Impact of historical climate change on the Southern Ocean carbon cycle, *J. Clim.*, *21*(22), 5820–5834, doi:10.1175/2008JCLI2194.1.

Mathot, S., W. O. S. Jr, C. A. Carlson, D. L. Garrison, M. M. Gowing, and C. L. Vickers (2000), Carbon partitioning within *Phaeocystis antarctica* (Prymnesiophyceae) colonies in the Ross Sea, Antarctica, *J. Phycol.*, *36*(6), 1049–1056, doi:10.1046/j.1529-8817.2000.99078.x.

McNeil, B. I., N. Metzl, R. M. Key, R. J. Matear, and A. Corbiere (2007), An empirical estimate of the Southern Ocean air-sea CO_2 flux, *Global Biogeochem. Cycles*, *21*, GB3011, doi:10.1029/2007GB002991.

Meredith, M. P., P. L. Woodworth, C. W. Hughes, and V. Stepanov (2004), Changes in the ocean transport through Drake Passage during the 1980s and 1990s, forced by changes in the Southern Annular Mode, *Geophys. Res. Lett.*, *31*, L21305, doi:10.1029/2004GL021169.

Metzl, N. (2009), Decadal increase of oceanic carbon dioxide in Southern Indian Ocean surface waters (1991–2007), *Deep Sea Res., Part II*, *56*(8–10), 607–619, doi:10.1016/j.dsr2.2008.12.007.

Metzl, N., C. Brunet, A. Jabaud-Jan, A. Poisson, and B. Schauer (2006), Summer and winter air-sea CO_2 fluxes in the Southern Ocean, *Deep Sea Res., Part I*, *53*(9), 1548–1563, doi:10.1016/j.dsr.2006.07.006.

Mikaloff Fletcher, S. E., et al. (2006), Inverse estimates of anthropogenic CO_2 uptake, transport, and storage by the ocean, *Global Biogeochem. Cycles*, *20*, GB2002, doi:10.1029/2005GB002530.

Mikaloff Fletcher, S. E., et al. (2007), Inverse estimates of the oceanic sources and sinks of natural CO_2 and the implied oceanic carbon transport, *Global Biogeochem. Cycles*, *21*, GB1010, doi:10.1029/2006GB002751.

Mongin, M. M., E. R. Abraham, and T. W. Trull (2009), Winter advection of iron can explain the summer phytoplankton bloom that extends 1000 km downstream of the Kerguelen Plateau in the Southern Ocean, *J. Mar. Res.*, *67*, 225–237, doi:10.1357/002224009789051218.

Montes-Hugo, M. A., M. Vernet, D. Martinson, R. Smith, and R. Iannuzzi (2008), Variability on phytoplankton size structure in the western Antarctic Peninsula (1997–2006), *Deep Sea Res., Part II*, *55*(18–19), 2106–2117, doi:10.1016/j.dsr2.2008.04.036.

Montes-Hugo, M., S. C. Doney, H. W. Ducklow, W. Fraser, D. Martinson, S. E. Stammerjohn, and O. Schofield (2009), Recent changes in phytoplankton communities associated with rapid regional climate change along the western Antarctic Peninsula, *Science*, *323*(5920), 1470–1473, doi:10.1126/science.1164533.

Moore, J. K., and M. R. Abbott (2000), Phytoplankton chlorophyll distributions and primary production in the Southern Ocean, *J. Geophys. Res.*, *105*(C12), 28,709–28,722, doi:10.1029/1999JC000043.

Moore, J. K., and O. Braucher (2008), Sedimentary and mineral dust sources of dissolved iron to the world ocean, *Biogeosciences*, *5*(3), 631–656, doi:10.5194/bg-5-631-2008.

Moore, J. K., S. C. Doney, J. A. Kleypas, D. M. Glover, and I. Y. Fung (2002), An intermediate complexity marine ecosystem model for the global domain, *Deep Sea Res., Part II*, *49*(1–3), 403–462, doi:10.1016/S0967-0645(01)00108-4.

Moore, J. K., S. C. Doney, and K. Lindsay (2004), Upper ocean ecosystem dynamics and iron cycling in a global three-dimensional model, *Global Biogeochem. Cycles*, *18*, GB4028, doi:10.1029/2004GB002220.

Moore, J. K., S. C. Doney, K. Lindsay, N. Mahowald, and A. F. Michaels (2006), Nitrogen fixation amplifies the ocean biogeochemical response to decadal timescale variations in mineral dust deposition, *Tellus, Ser. B*, *58*(5), 560–572, doi:10.1111/j.1600-0889.2006.00209.x.

Park, Y.-H., F. Roquet, I. Durand, and J.-L. Fuda (2008), Large-scale circulation over and around the Northern Kerguelen Plateau, *Deep Sea Res., Part II*, *55*(5–7), 566–581, doi:10.1016/j.dsr2.2007.12.030.

Patra, P. K., J. K. Moore, N. Mahowald, M. Uematsu, S. C. Doney, and T. Nakazawa (2007), Exploring the sensitivity of interannual basin-scale air-sea CO_2 fluxes to variability in atmospheric dust deposition using ocean carbon cycle models and atmospheric CO_2 inversions, *J. Geophys. Res.*, *112*, G02012, doi:10.1029/2006JG000236.

Peloquin, J. A., and W. O. Smith Jr. (2007), Phytoplankton blooms in the Ross Sea, Antarctica: Interannual variability in magnitude, temporal patterns, and composition, *J. Geophys. Res.*, *112*, C08013, doi:10.1029/2006JC003816.

Pollard, R. T., H. J. Venables, J. F. Read, and J. T. Allen (2007), Large-scale circulation around the Crozet Plateau controls an annual phytoplankton bloom in the Crozet Basin, *Deep Sea Res., Part II*, *54*(18–20), 1915–1929, doi:10.1016/j.dsr2.2007.06.012.

Poulton, A. J., C. Mark Moore, S. Seeyave, M. I. Lucas, S. Fielding, and P. Ward (2007), Phytoplankton community composition around the Crozet Plateau, with emphasis on diatoms and *Phaeocystis*, *Deep Sea Res., Part II*, *54*(18–20), 2085–2105, doi:10.1016/j.dsr2.2007.06.005.

Prézelin, B. B., E. E. Hofmann, M. Moline, and J. M. Klinck (2004), Physical forcing of phytoplankton community structure and primary production in continental shelf waters of the Western Antarctic Peninsula, *J. Mar. Res.*, *62*, 419–460, doi:10.1357/0022240041446173.

Ross, R. M., L. B. Quetin, D. G. Martinson, R. A. Iannuzzi, S. E. Stammerjohn, and R. C. Smith (2008), Palmer LTER: Patterns of distribution of five dominant zooplankton species in the epipelagic zone west of the Antarctic Peninsula, 1993–2004, *Deep Sea Res., Part II*, *55*(18–19), 2086–2105, doi:10.1016/j.dsr2.2008.04.037.

Roy, T., P. Rayner, R. Matear, and R. Francey (2003), Southern Hemisphere ocean CO_2 uptake: Reconciling atmospheric and oceanic estimates, *Tellus, Ser. B*, *55*(2), 701–710, doi:10.1034/j.1600-0889.2003.00058.x.

Sabine, C. L., et al. (2004), The oceanic sink for anthropogenic CO_2, *Science*, *305*(5682), 367–371, doi:10.1126/science.1097403.

Santer, B. D., T. M. L. Wigley, J. S. Boyle, D. J. Gaffen, J. J. Hnilo, D. Nychka, D. E. Parker, and K. E. Taylor (2000), Statistical significance of trends and trend differences in layer-average atmospheric temperature time series, *J. Geophys. Res.*, *105*(D6), 7337–7356, doi:10.1029/1999JD901105.

Sarmiento, J. L., N. Gruber, M. A. Brzezinski, and J. P. Dunne (2004), High-latitude controls of thermocline nutrients and low latitude biological productivity, *Nature*, *427*(6969), 56–60, doi:10.1038/nature02127.

Smith, W. O., Jr., and V. L. Asper (2001), The influence of phytoplankton assemblage composition on biogeochemical characteristics and cycles in the southern Ross Sea, Antarctica, *Deep Sea Res., Part I*, *48*(1), 137–161, doi:10.1016/S0967-0637(00)00045-5.

Smith, W. O., Jr., and J. C. Comiso (2008), Influence of sea ice on primary production in the Southern Ocean: A satellite perspective, *J. Geophys. Res.*, *113*, C05S93, doi:10.1029/2007JC004251.

Smith, W. O., Jr., D. Nelson, and S. Mathot (1999), Phytoplankton growth rates in the Ross Sea, Antarctica, determined by independent methods: Temporal variations, *J. Plankton Res.*, *21*(8), 1519–1536, doi:10.1093/plankt/21.8.1519.

Smith, R. C., D. G. Martinson, S. E. Stammerjohn, R. A. Iannuzzi, and K. Ireson (2008), Bellingshausen and western Antarctic Peninsula region: Pigment biomass and sea-ice spatial/temporal distributions and interannual variability, *Deep Sea Res., Part II*, *55*(18–19), 1949–1963, doi:10.1016/j.dsr2.2008.04.027.

Stammerjohn, S. E., D. G. Martinson, R. C. Smith, and R. A. Iannuzzi (2008), Sea ice in the western Antarctic Peninsula region: Spatio-temporal variability from ecological and climate change perspectives, *Deep Sea Res., Part II*, *55*(18–19), 2041–2058, doi:10.1016/j.dsr2.2008.04.026.

Tagliabue, A., et al. (2010), Hydrothermal contribution to the oceanic dissolved iron inventory, *Nat. Geosci.*, *3*(4), 252–256, doi:10.1038/ngeo818.

Takahashi, T., et al. (2009), Climatological mean and decadal change in surface ocean pCO_2, and net sea-air CO_2 flux over the global oceans, *Deep Sea Res., Part II*, *56*(8–10), 554–577, doi:10.1016/j.dsr2.2008.12.009.

Tang, K. W., W. O. Smith, A. R. Shields, and D. T. Elliott (2009), Survival and recovery of *Phaeocystis antarctica* (Prymnesiophyceae) from prolonged darkness and freezing, *Proc. R. Soc. London, Ser. B*, *276*(1654), 81–90, doi:10.1098/rspb.2008.0598.

Thompson, D. W. J., and S. Solomon (2002), Interpretation of recent Southern Hemisphere climate change, *Science*, *296*(5569), 895–899, doi:10.1126/science.1069270.

Thompson, D. W. J., J. M. Wallace, and G. C. Hegerl (2000), Annular modes in the extratropical circulation. Part II: Trends, *J. Clim.*, *13*(5), 1018–1036, doi:10.1175/1520-0442(2000)013<1018:AMITEC>2.0.CO;2.

Toggweiler, J. R., K. Dixon, and W. S. Broecker (1991), The Peru upwelling and the ventilation of the South Pacific thermocline, *J. Geophys. Res.*, *96*(C11), 20,467–20,497, doi:10.1029/91JC02063.

Turner, J., S. R. Colwell, G. J. Marshall, T. A. Lachlan-Cope, A. M. Carleton, P. D. Jones, V. Lagun, P. A. Reid, and S. Iagovkina (2005), Antarctic climate change during the last 50 years, *Int. J. Climatol.*, *25*(3), 279–294, doi:10.1002/joc.1130.

Vernet, M., D. Martinson, R. Iannuzzi, S. Stammerjohn, W. Kozlowski, K. Sines, R. Smith, and I. Garibotti (2008), Primary production within the sea-ice zone west of the Antarctic Peninsula: I. Sea ice, summer mixed layer, and irradiance, *Deep Sea Res., Part II*, *55*(18–19), 2068–2085, doi:10.1016/j.dsr2.2008.05.021.

Wagener, T., C. Guieu, R. Losno, S. Bonnet, and N. Mahowald (2008), Revisiting atmospheric dust export to the Southern Hemisphere ocean: Biogeochemical implications, *Global Biogeochem. Cycles*, *22*, GB2006, doi:10.1029/2007GB002984.

Wang, S., and J. K. Moore (2011), Incorporating *Phaeocystis* into a Southern Ocean ecosystem model, *J. Geophys. Res.*, *116*, C01019, doi:10.1029/2009JC005817.

Ward, P., M. Whitehouse, R. Shreeve, S. Thorpe, A. Atkinson, R. Korb, D. Pond, and E. Young (2007), Plankton community structure south and west of South Georgia (Southern Ocean): Links with production and physical forcing, *Deep Sea Res., Part I*, *54*(11), 1871–1889, doi:10.1016/j.dsr.2007.08.008.

Wetzel, P., A. Winguth, and E. Maier-Reimer (2005), Sea-to-air CO_2 flux from 1948 to 2003: A model study, *Global Biogeochem. Cycles*, *19*, GB2005, doi:10.1029/2004GB002339.

Yeager, S. G., C. A. Shields, W. G. Large, and J. J. Hack (2006), The low-resolution CCSM3, *J. Clim.*, *19*(11), 2545–2566, doi:10.1175/JCLI3744.1.

J. K. Moore and S. Wang, Earth System Science, University of California, Irvine, Croul Hall 1101D, Irvine, CA 92697, USA. (shanlinw@uci.edu)